

Quantized Iterative Learning Control of Communication Constrained Systems with Encoding and Decoding Mechanism

Yujuan Tao*, Hongfeng Tao, Zhihe Zhuang, Vladimir Stojanovic[†], Wojciech Paszke[‡]

22.12.2023

Abstract

In practical applications, due to the limited communication bandwidth, the network control systems (NCSs) are prone to data dropouts when the load is high. In this paper, the problem of quantized iterative learning control (ILC) based on encoding and decoding mechanism for such communication constrained systems is studied. By combining the encoding and decoding mechanism with the uniform quantizer, the network burden and the impact of quantization error on the tracking performance of the systems are significantly mitigated. Meanwhile, data dropouts are represented as the Bernoulli random variable model, and an ILC law based on gradient is designed. When data dropouts occur, the signals maintain the value of the previous trial, otherwise the signals are updated. For this kind of learning framework, the asymptotic zero-error tracking performance has been rigorously proven for the uniform quantizer. To validate the proposed design, a joint motion of an industrial robot in the horizontal plane is simulated as an example.

Iterative Learning Control, Communication Constrained Systems, Encoding and Decoding Mechanism, Uniform Quantizer, Data Dropouts.

1 Introduction

Iterative learning control (ILC), as a control method with obvious advantages for repetitive control systems, has been widely studied and applied since it was first applied to robot systems in [Arimoto et al. \(1984\)](#). Compared with the traditional control methods which focus more on the time axis, the basic principle of ILC is to improve the performance of the system by adding the previous trials' information to the current trial and constantly updating its information, so as to achieve

*Key Laboratory of Advanced Process Control for Light Industry (Ministry of Education), Jiangnan University, China

[†]Department of Automatic Control, Robotics and Fluid Technique, Faculty of Mechanical and Civil Engineering, University of Kragujevac, Serbia

[‡]Institute of Automation, Electronic and Electrical Engineering, University of Zielona Gó'ra, Poland

the perfect tracking of the expected trajectory of the system output. Due to the repeatability of ILC, it is widely used in many control systems in repetitive operation modes, such as chemical batch processes (Shibani et al. (2023)), robot systems (Guan et al. (2023)), urban traffic network systems (Ren et al. (2020)) and printer conveyor drive systems (Wang et al. (2020)), etc.

The development of communication technology promotes the combination of network and control systems, and networked control systems (NCSs) have become a focus of extensive research and examination (Yang et al. (2020);Liu et al. (2021);Bahreini et al. (2022);Yu and Chen. (2023)). Compared to traditional control systems, the network control mode offers several advantages, which is easy to be maintained and connected, and has high efficiency. However, with the current communication technology, given the diverse factors at play, including actual conditions and the field environment, communication constraints can result in a loss of data transmission accuracy, leading to challenges such as data dropouts, communication delays, and variations in trajectory lengths. Therefore, ensuring the timeliness and reliability of network communication has become a crucial research in NCSs area. Quantization discretizes the data, which can effectively reduce the amount of data transmitted by the network. To name a few, in Li et al (2021), a new asynchronous event-triggered communication strategy was proposed under the quantization of the transmission signals, which effectively reduced the network communication burden of the communication channel. The observer-based quantized output feedback control for a class of nonlinear discrete-time systems was studied in Chang and Jin (2022). All transmitted signals in the closed-loop system were quantized by a dynamic quantizer to ensure the tracking performance of the quantized closed-loop system. These studies prompt us to combine ILC with quantitative mechanisms.

Since Bu et al. (2015) first studied the quantization problem in ILC, quantization has long been introduced into ILC. Quantization is bound to bring quantization error and reduce the accuracy of data transmission, thus affecting control performance. To mitigate the impact of quantization error on the control systems, Xu et al. (2017) used adaptive improvement of the logarithmic quantizer to quantify the quantization error based on the sector boundary method, so as to achieve accurate tracking performance. In Bu et al. (2017), the same quantizer was utilized to quantize the input, output, and tracking error signals. Finally, the quantization of the input and output signals is verified, so that the system tracking error converges to a bounded value. And the boundary is influenced by the quantization density and the tracking trajectory. Moreover, the quantization of tracking error makes zero-error tracking possible. It is noted that based on the inherent characteristics of the logarithmic quantizer, zero-error convergence performance can be achieved. However, is there any way to reduce the impact of quantization error for other quantizers?

In Gao et al. (2017), by using dynamic encoding/decoding technology and distributed event-triggered strategy, a bit quantization scheme was proposed to achieve asymptotic consensus in multi-agent systems that had limited communication rates. In Zhang and Shen. (2018), the quantization scheme combining the encoding and decoding mechanism with the uniform quantizer was introduced into the ILC. The output signals were quantized, encoded and transmitted, and then the input signals were updated. Finally, it was verified that the desired trajectory can be accurately tracked under this mechanism. Subsequently, Shen and Zhang. (2022) extended this method to quantize signals on both the measurement side and the actuator side, which also can achieve zero-error tracking. Under this mechanism, Zhang et al. (2022) proposed an E-DM-based quantized data-driven ILC method. This method ensured the zero-error convergence of the iterative domain. Therefore, studying signal quantization ILC law based on this mechanism can help improve system

performance. This paper also uses the method of combining quantizer with encoding and decoding mechanism to carry out research.

With the application of ILC strategy in NCSs, the controller and the controlled object are transmitted by the network. Due to the problems of long transmission distance, limited bandwidth, and vulnerability to network interference and attack, the network often leads to data dropouts or delay of data transmission. In practical applications, the impact of communication constraints cannot be ignored. Therefore, the ILC design in this paper considers the tracking task in the data dropouts environment. The research on unstable network control has attracted more and more scholars' attention. To name a few, [Shen et al. \(2016\)](#) analyzed the convergence of ILC in linear stochastic systems under the general data dropouts environment. Data dropouts occurred randomly on the measurement side and the actuator side. With the help of Markov model, a new analysis method was developed, which independently updated the calculated input and the actual input, to achieve tracking error convergence in the terms of mean square and almost certain sense. [Huang et al. \(2019\)](#) studied the compensation problem for data dropouts in the time domain and iterative domain, introduced an input error transfer matrix on the actuator side, and finally verified that only compensation in the iterative domain can ensure that the output error converges to zero. In the case of data dropouts and channel noise on both the measurement side and the actuator side, an optimal input filter was developed to estimate the updated input of the controller, which theoretically ensured the convergence performance of the filtering error covariance matrix in [Huang et al. \(2022\)](#). The focus of this paper is whether the designed algorithm is effective for systems with data dropouts. Therefore, similar to [Shen and Xu. \(2017\)](#); [Tang and Sheng. \(2018\)](#); [Zhang et al. \(2019\)](#), data dropouts are described by random variables satisfying Bernoulli distributions in this paper.

Motivated by the above previous studies, this paper designs an optimal ILC algorithm for linear time-invariant systems with different data dropouts rates under input and output signals quantization. By comparing two different quantization strategies, it is verified that the encoding and decoding mechanism can effectively reduce the impact of quantization error, and realize the monotonic convergence of tracking error in the sense of mathematical expectation. The influence of different data dropouts rates on the convergence performance of the system is analyzed. By taking a joint motion of an industrial robot in the horizontal plane as an example, the effectiveness of the algorithm is verified.

In summary, this paper presents the following main contributions:

- Under the framework of the lifted system, the input and output signals are quantized by combining the encoding and decoding mechanism with the uniform quantizer. The ILC law is designed by using the gradient method to realize the accurate tracking of the desired trajectory. This work promotes the study of ILC with data dropouts and signals quantization.
- Compared with the uniform quantizer directly quantifying system signals, the designed quantized ILC law can effectively reduce the influence of quantization error on tracking performance and achieve monotonic convergence under mathematical expectation.

The following sections outline the organization of this paper: Section “Problem Formulation” gives the problem formulation of random data dropouts problem for linear discrete-time systems and the quantized control strategies. In section “ILC Design”, the ILC laws of two control strategies are given and the tracking error convergence is proved. In section “Simulation”, the simulations are presented to demonstrate the effectiveness of the proposed algorithm. Following that, in section “Conclusion”, a comprehensive summary of the entire study is provided.

2 Problem Formulation

Considering a single-input single-output linear discrete time-invariant systems as follows

$$\begin{cases} x_k(t+1) = Ax_k(t) + Bu_k(t) \\ y_k(t) = Cx_k(t) \end{cases} \quad (1)$$

where the subscript k denotes the trial number, $k = 0, 1, \dots, \infty$; $t \in [0, N]$ is the time index and N denotes the trial length; Denote by $y_k(t) \in \mathbb{R}$, $u_k(t) \in \mathbb{R}$, $x_k(t) \in \mathbb{R}^n$ the output, input and state of the system, severally; The parameter matrices of the system are composed of A , B , C with corresponding dimensions. Assuming that $CB \neq 0$ to ensure the system is controllable. The initial state is assumed, not lose its generality, to be the same for each trial and $x_k(0)$ represents the initial condition of the system at k th trial.

In practical applications, the state signals of the system is often complex or difficult to observe, so the state quantization based ILC design has certain limitations. This paper only considers the quantization of input and output signals. For the linear discrete-time system (1), the state space model is transformed into super vector form by using lifting technique

$$y_{k+1} = Hu_{k+1} + d_{k+1} \quad (2)$$

where

$$u_k = [u_k(0), u_k(1), \dots, u_k(N-1)]^T \quad (3)$$

$$y_k = [y_k(1), y_k(2), \dots, y_k(N)]^T \quad (4)$$

and H and d_k represent the system model transfer matrix and the influence of initial conditions respectively, i.e.,

$$H = \begin{bmatrix} CB & 0 & \dots & 0 \\ CAB & CB & \dots & 0 \\ \vdots & \vdots & \ddots & \vdots \\ CA^{N-1}B & CA^{N-2}B & \dots & CB \end{bmatrix} \quad (5)$$

$$d_k = [CA, CA^2, CA^3, \dots, CA^N]^T x_k(0) \quad (6)$$

The control objective of the ILC is to design a control law u_{k+1} for the desired trajectory y_d , such that the output sequence of the system can converge to y_d at $k \rightarrow \infty$, and the actual tracking error is set to $e_k = y_d - y_k$. The following assumptions need to be introduced to facilitate the design of ILC law.

Assumption 1. (Patan et al. (2020)) *There exists an expected trajectory y_d , whose state space model in ILC is*

$$\begin{cases} x_d(t+1) = Ax_d(t) + Bu_d(t) \\ y_d(t) = Cx_d(t) \end{cases} \quad (7)$$

where $u_d(t)$ denotes the expected input, and the expected system state is represented by $x_d(t)$.

Assumption 2. (Patan et al. (2020)) *Assuming no loss of generality, the initial conditions of the system are the same as the expected initial conditions, which are set to*

$$x_k(0) = x_d(0) = 0 \quad (8)$$

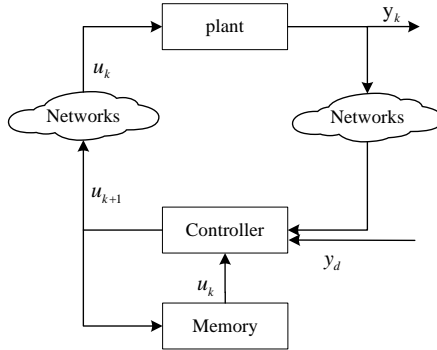


Figure 1: The block diagram of network control systems.

where $x_d(0)$ represents the initial expected state value of the system.

Since it is assumed $x_k(0) = 0$, then $d_k = 0$. System (2) can be converted to

$$y_{k+1} = H u_{k+1} \quad (9)$$

The distribution of the NCSs is illustrated in Fig.1. The plant and the controller are transmitted via the network. The desired trajectory is first sent to the system to generate tracking errors, which are transmitted to the controller for iterative update. The output signals of the system are transmitted to the controller through the network, and then the input signals generated by the controller are transmitted back to the controlled system via the network to form a closed loop. In order to reduce the network burden caused by communication constraints, this paper considers the quantization of input and output signals. And a uniform quantizer in [Choi and Yoo. \(2020\)](#) is used:

$$Q(m) = \begin{cases} 0, & -1 < m \leq 1 \\ 2i, & 2i - 1 < m \leq 2i + 1 \\ 2v, & m > 2v - 1 \\ -Q(-m), & m \leq -1 \end{cases} \quad (10)$$

where $i = 0, 1, \dots, v - 1$, $i \in \mathbb{Z}^+$, denotes the quantization level, v denotes the maximum quantization level. Denote by m the input of the quantizer, when the input of the quantizer satisfies $m \leq 2v - 1$, the input and output of the quantizer satisfy

$$\eta = q(m) - m \quad (11)$$

where η represents the quantization error, satisfying $|\eta| \leq 1$.

On account of the limited quantization ability of the uniform quantizer, the quantization error will be brought. To mitigate the impact of quantization error on the system, an encoding and decoding mechanism is employed to further improve the tracking performance of the system. Here two quantization schemes are used: one is to directly quantize the input and output signals, and the other is to combine the quantizer with the encoding and decoding mechanism to quantize the input and output signals. Fig. 2 shows the block diagram of NCSs based on encoding and decoding mechanism. The E1, D1 and E2, D2 blocks represent the input encoder and decoder, the output encoder and decoder, respectively. The output signals are encoded by the encoder E2 and transmitted through the network to the decoder D2 for decoding, and then transmitted to the

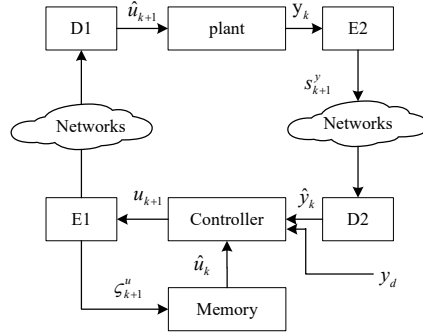


Figure 2: Network control system block diagram of the proposed ILC scheme.

controller to generate the input signals. The generated input signals are transmitted in the same way as the output signals. The input encoder E1 and decoder D1 based on uniform quantizer are designed as below

$$\begin{cases} \varsigma_0^u(t) = 0 \\ s_{k+1}^u(t) = Q\left(\frac{u_{k+1}(t) - \varsigma_k^u(t)}{b_k}\right) \\ \varsigma_{k+1}^u(t) = b_k s_{k+1}^u(t) + \varsigma_k^u(t) \end{cases} \quad (12)$$

and

$$\begin{cases} \hat{u}_0(t) = 0 \\ \hat{u}_{k+1}(t) = b_k s_{k+1}^u(t) + \hat{u}_k(t) \end{cases} \quad (13)$$

where $\varsigma_k^u(t)$, $u_k(t)$, $s_{k+1}^u(t)$ represent the internal state, input and output of the encoder E1 respectively, and $b_k = \tau^k$ denotes the regulatory sequence used to improve the tracking effect. $\hat{u}_k(t)$ is the output of the decoder D1 and represents the measured input signals of the system.

The situation that the output signals are quantized by the quantizer and transmitted through an unstable network is considered, and random data dropouts occur during transmission. Suppose that encoder and decoder can detect whether the data is lost or not. Once the data dropouts occur, the encoder and decoder respond immediately. Combining data dropouts to design the output encoder E2 and decoder D2. Similarly, based on the uniform quantizer, the output encoder E2 and decoder D2 are designed as follows

$$\begin{cases} \varsigma_0^y(t) = 0 \\ s_{k+1}^y(t) = Q\left(\frac{y_{k+1}(t) - \varsigma_k^y(t)}{b_{k+1}}\right) \\ \varsigma_{k+1}^y(t) = b_{k+1} w_{k+1}(t) s_{k+1}^y(t) + \varsigma_k^y(t) \end{cases} \quad (14)$$

and

$$\begin{cases} \hat{y}_0(t) = 0 \\ \hat{y}_{k+1}(t) = b_{k+1} w_{k+1}(t) s_{k+1}^y(t) + \hat{y}_k(t) \end{cases} \quad (15)$$

where $\varsigma_k^y(t)$, $y_k(t)$, $s_{k+1}^y(t)$ represent the internal state, input and output of the encoder E2 respectively. $\hat{y}_k(t)$ is the output of the decoder and represents the measured output signal of the system. $w_{k+1}(t)$ is used to determine whether the output signals are successfully transmitted. $w_{k+1}(t) = 1$ means that the data is successfully transmitted, otherwise $w_{k+1}(t) = 0$. Similar to [Shen and Xu. \(2017\)](#), the Bernoulli variables are used to model the data dropouts. Without losing generality,

$$P\{w_{k+1}(t) = 1\} = \omega_t, P\{w_{k+1}(t) = 0\} = 1 - \omega_t \quad (16)$$

where $0 < \omega_t < 1$, represents the probability of successful transmission of the output signals.

Remark 1. The data dropouts are independent on the iteration axis, then, $\lim_{n \rightarrow \infty} \frac{1}{n} [\sum_{k=1}^n \omega_k(t)] = \omega_t$. If $\omega_t = 0$, the data must be lost, indicating that the controller can not get any information from the controlled system, thus, the algorithm can not be used to improve the performance of the system. If $\omega_t = 1$, there is no data dropouts occurring. With the design of ILC law in the case of data dropouts, we assume that $0 < \omega_t < 1$. Moreover, for the time point t , the data dropouts probability of different trials k is unknown and fixed. It can be obtained that $w_{k+1}(t)$ is a time-related variable, that is, $E\{w_{k+1}(t)\} = \omega_t$.

After the input signals are quantized, the actual system input sequence is replaced by \hat{u}_{k+1} , and the form of system (9) can be converted into

$$y_{k+1} = H\hat{u}_{k+1} \quad (17)$$

The relationship between the actual input signals and the measured input signals is considered before designing the control law. Substituting $s_{k+1}^u(t)$ in (12) into (13), it can be obtained that

$$\begin{aligned} \hat{u}_{k+1}(t) &= b_k s_{k+1}^u(t) + \hat{u}_k(t) \\ &= b_k Q\left(\frac{u_{k+1}(t) - \varsigma_k^u(t)}{b_k}\right) + \hat{u}_k(t) \\ &= b_k \left(\frac{u_{k+1}(t) - \varsigma_k^u(t)}{b_k} + \eta_{k+1}^u(t)\right) + \hat{u}_k(t) \\ &= u_{k+1}(t) + b_k \eta_{k+1}^u(t) + \hat{u}_k(t) - \varsigma_k^u(t) \end{aligned} \quad (18)$$

where $\eta_{k+1}^u = Q\left(\frac{u_{k+1}(t) - \varsigma_k^u(t)}{b_k}\right) - \frac{u_{k+1}(t) - \varsigma_k^u(t)}{b_k}$, denotes the quantization error of the input signals.

Lemma 1. The term $\hat{u}_k(t) - \varsigma_k^u(t)$ in (18) satisfies $\hat{u}_k(t) - \varsigma_k^u(t) = 0, \forall k$.

Proof. The proof is shown in Zhang et al. (2014).

Combining (18) and Lemma 1, the relationship between the output of the system controller and its measured value can be obtained as

$$\hat{u}_{k+1}(t) = u_{k+1}(t) + b_k \eta_{k+1}^u(t) \quad (19)$$

To facilitate the design of the system ILC update law, the system input sequence and the generated input sequence are reconstructed as super vectors

$$\hat{u}_{k+1} = u_{k+1} + b_k \eta_{k+1}^u \quad (20)$$

Similarly, the relationship between the actual output signals and the estimated output signals can be derived

$$\begin{aligned} \hat{y}_{k+1}(t) &= b_{k+1} w_{k+1}(t) s_{k+1}^y(t) + \hat{y}_k(t) \\ &= b_{k+1} w_{k+1}(t) Q\left(\frac{y_{k+1}(t) - \varsigma_k^y(t)}{b_{k+1}}\right) + \hat{y}_k(t) \\ &= b_{k+1} w_{k+1}(t) \eta_{k+1}^y(t) + w_{k+1}(t) (y_{k+1}(t) - \varsigma_k^y(t)) + \hat{y}_k(t) \end{aligned} \quad (21)$$

where $\eta_{k+1}^y = Q\left(\frac{y_{k+1}(t) - \varsigma_k^y(t)}{b_{k+1}}\right) - \frac{y_{k+1}(t) - \varsigma_k^y(t)}{b_{k+1}}$ denotes the quantization error of the output signals. Then the system output sequence and the generated output sequence are reconstructed as super vectors

$$\hat{y}_{k+1} = \mathcal{M}_{k+1} [y_{k+1} + b_{k+1} \eta_{k+1}^y] + \bar{\mathcal{M}}_{k+1} \hat{y}_k \quad (22)$$

where $\mathcal{M}_{k+1} = \text{diag}(w_{k+1}(0), w_{k+1}(1), \dots, w_{k+1}(N-1))$, $\bar{\mathcal{M}}_{k+1} = \text{diag}(1 - w_{k+1}(0), \dots, 1 - w_{k+1}(N-1))$, thus, $\mathcal{M}_{k+1} + \bar{\mathcal{M}}_{k+1} = I$. As indicated by equation (22), when the data is lost, the system maintains the value of the previous trial for transmission, otherwise the system is updated.

3 ILC Design

In this section, two ILC laws are proposed to achieve control objectives in data dropouts environment. One is obtained by directly quantifying the signals by the uniform quantizer, and the other is obtained by quantifying the signals based on the encoding and decoding mechanism. Both of them are based on the gradient descent method and are obtained by minimizing the following norm optimization cost function

$$J(u_k) = \|e_k\|^2 \quad (23)$$

where $e_k = y_d - y_k$ is the tracking error at k th trial, and the induced norm $\|e_k\|^2 = e_k^T e_k$ is defined.

The control law is obtained by minimizing the cost function (23) with respect to u_k

$$u_{k+1} = u_k - \beta \frac{\partial J(u_k)}{\partial u_k} \quad (24)$$

where β is a positive scalar gain. The system tracking error is added to the ILC update law, and it is iteratively reduced under the ILC framework to finally achieve accurate tracking.

3.1 Quantifying the Input and Output Signals Based on Encoding and Decoding Mechanism

In order to consider the quantization error caused by quantization output and the impact of data dropouts, the cost function (23) is modified as

$$J(u_k) = \frac{1}{4} \|\hat{e}_k\|^2 \quad (25)$$

where $\hat{e}_k = y_d - \hat{y}_k$, denotes the measured error caused by quantization, and it is obtained by (22). To derive the ILC law, the following result is required.

Proposition 1. *The ILC law is obtained by minimizing the cost function (25) with respect to u_k*

$$u_{k+1} = \hat{u}_k + \beta H^T \mathcal{M}_k (\hat{e}_k + H b_{k-1} \eta_k^u + b_k \eta_k^y) \quad (26)$$

Proof 1. By (22), it can be obtained that

$$\begin{aligned} \hat{e}_k &= y_d - \hat{y}_k = y_d - \mathcal{M}_k (y_k + b_k \eta_k^y) - \bar{\mathcal{M}}_k \hat{y}_{k-1} \\ &= y_d - \mathcal{M}_k (H u_k + H b_{k-1} \eta_k^u + b_k \eta_k^y) - \bar{\mathcal{M}}_k \hat{y}_{k-1} \end{aligned} \quad (27)$$

then, (25) is converted to

$$\begin{aligned} J(u_k) &= \frac{1}{4} \left\| y_d - \mathcal{M}_k (H u_k + H b_{k-1} \eta_k^u + b_k \eta_k^y) - \bar{\mathcal{M}}_k \hat{y}_{k-1} \right\|^2 \\ &\leq \frac{1}{4} \left(\left\| y_d - \mathcal{M}_k H u_k - \bar{\mathcal{M}}_k \hat{y}_{k-1} \right\| + \left\| \mathcal{M}_k H b_{k-1} \eta_k^u + b_k \mathcal{M}_k \eta_k^y \right\| \right)^2 \\ &\leq \frac{1}{2} \left\| y_d - \mathcal{M}_k H u_k - \bar{\mathcal{M}}_k \hat{y}_{k-1} \right\|^2 + \frac{1}{2} \left\| \mathcal{M}_k H b_{k-1} \eta_k^u + b_k \mathcal{M}_k \eta_k^y \right\|^2 \\ &\leq \frac{1}{2} \left\| y_d - \mathcal{M}_k H u_k - \bar{\mathcal{M}}_k \hat{y}_{k-1} \right\|^2 + \frac{1}{2} \|H \mathcal{M}_k\|^2 N b_{k-1} + \frac{1}{2} N \|\mathcal{M}_k\|^2 b_k \end{aligned} \quad (28)$$

Algorithm 1. quantifying signals based on encoding and decoding mechanism

- Step 1.** (Initialization) The initial input signals are $u_0 = 0$; the initial output signals are $y_0 = 0$; the initial state value is $x_0 = 0$, so the initial error of the system is $e_0 = y_d - y_0 = y_d$; Γ represents the maximum number of trials; set $k = 1$.
- Step 2.** (Optimization) Perform the following steps to obtain the input u_{k+1} .
- (a) using (12) to calculate s_k^u and update ς_k^u ;
 - (b) applying s_k^u to (13) to get the measurement input \hat{u}_k ;
 - (c) applying \hat{u}_k to (17) to get the actual output y_k ;
 - (d) using (14) to calculate s_k^y and update ς_k^y ;
 - (e) applying s_k^y to (15) to get the measurement output \hat{y}_k ;
 - (f) applying \hat{y}_k to (26) to update ILC law u_{k+1} .
- Step 3.** (Updating) Let $k = k + 1$ and repeat Step 2. until the end condition is satisfied.
-

therefore, a new cost function $J_1(u_k)$ can be obtained

$$J_1(u_k) = \frac{1}{2} \|y_d - \mathcal{M}_k H u_k - \bar{\mathcal{M}}_k \hat{y}_{k-1}\|^2 + \varepsilon_k \quad (29)$$

where $\varepsilon_k = \frac{1}{2\tau} \|H\mathcal{M}_k\|^2 N b_k + \frac{1}{2} N \|\mathcal{M}_k\|^2 b_k$ is independent of u_k .

The cost function is differentiated by u_k to obtain

$$\begin{aligned} \frac{\partial J_1(u_k)}{\partial u_k} &= -H^T \mathcal{M}_k (y_d - \mathcal{M}_k H u_k - \bar{\mathcal{M}}_k \hat{y}_{k-1}) \\ &= -H^T \mathcal{M}_k (\hat{e}_k + \mathcal{M}_k H b_{k-1} \eta_k^u + \mathcal{M}_k b_k \eta_k^y) \end{aligned} \quad (30)$$

where $\mathcal{M}_k^T = \mathcal{M}_k$ is a diagonal matrix.

The ILC law is obtained from (30)

$$u_{k+1} = \hat{u}_k + \beta H^T \mathcal{M}_k (\hat{e}_k + H b_{k-1} \eta_k^u + b_k \eta_k^y) \quad (31)$$

which completes the proof.

Remark 2. \mathcal{M}_k is a diagonal matrix of 0 – 1 Bernoulli binary variables with probability ω_t , where ω_t represents the data dropouts rate. According to $\bar{\mathcal{M}}_k = I - \mathcal{M}_k$, it can be concluded that $\mathcal{M}_k \bar{\mathcal{M}}_k = 0$ and $\mathcal{M}_k \mathcal{M}_k = \mathcal{M}_k$.

It can be seen from Algorithm 1 that the output signals y_k are first quantized, encoded and decoded to obtain the measured output signals \hat{y}_k , which are transmitted to the controller to update the input signals u_{k+1} , and then the input signals u_{k+1} are subjected to the same operation to obtain the measured input signals \hat{u}_{k+1} to optimize the system performance. The process can be expressed as $y_k \rightarrow \hat{y}_k \rightarrow u_{k+1} \rightarrow \hat{u}_{k+1}$.

Through (31), it can be seen that the ILC law contains the product term of the quantization error and the adjustment sequence b_k . Selecting the appropriate adjustment sequence can make the item asymptotically converge to zero. The controller continuously modifies the input signals through the ILC control law to reduce the quantization error, which can ultimately realize zero-error tracking. This is summarized by Theorem 1.

Theorem 1. *Considering the system (17) with the ILC law (31) based on encoding and decoding mechanism, the expected norm of the tracking error converges to zero if it satisfies*

$$\|I - \beta HH^T P\| \leq \rho_1 < 1 \quad (32)$$

where $P = E\{\mathcal{M}_K\} = \text{diag}\{\omega_0, \omega_1, \dots, \omega_{N-1}\}$, and ρ_1 is a constant, then the learning gain step β satisfies

$$0 < \beta < \frac{2}{\|HH^T\|} \quad (33)$$

Proof 2. See Appendix.

The analysis demonstrates that the proposed ILC law can achieve the convergence of the system tracking error in the sense of the expected norm, that is, the proposed algorithm can achieve accurate trajectory tracking.

3.2 Quantifying the Input and Output Signals Without Encoding and Decoding Mechanism

This paper only focuses on the advantages of the output signals with the proposed design compared with the direct quantization method in the data dropouts environment. Under the direct quantization method, the relationship between the system output signals and the estimated output signals can be derived to

$$\hat{y}_{k+1}^p(t) = Q(y_{k+1}(t)) = y_{k+1}(t) + \eta_{k+1}^p(t) \quad (34)$$

where $\eta_{k+1}^p(t) = Q(y_{k+1}(t)) - y_{k+1}(t)$, represents the direct quantization error of the system output signals. The output signals of the system are quantized by the quantizer and transmitted to the controller through an unstable network, and the estimated output signals (34) can be converted into

$$\hat{y}_{k+1}^q(t) = w_{k+1}(t)\hat{y}_{k+1}^p(t) + (1 - w_{k+1}(t))\hat{y}_k^p(t) \quad (35)$$

converting (35) into super vector

$$\hat{y}_{k+1}^q = \mathcal{M}_{k+1}\hat{y}_{k+1}^p + \bar{\mathcal{M}}_{k+1}\hat{y}_k^p \quad (36)$$

using the same method as the proposed ILC design, for quantifying signals directly, the cost function is

$$J^p(u_k) = \frac{1}{4} \|\hat{e}_k^p\|^2 \quad (37)$$

where $\hat{e}_k^p = y_d - \hat{y}_k^q$ denotes the quantization error of the output signals, $\|\hat{e}_k^p\|^2 = (\hat{e}_k^p)^T \hat{e}_k^p$.

Proposition 2. *For the direct quantized output signal, the system ILC law is obtained by minimizing the cost function (37) with respect to u_k*

$$u_{k+1} = \hat{u}_k + \beta H^T \mathcal{M}_k (\hat{e}_k^p + H\eta_k^{pu} + \eta_k^p) \quad (38)$$

where $\eta_k^{pu} = Q(u_k) - u_k$ denotes the direct quantization error of the input signals.

Proof 3. By (34) and (36), it can be obtained

$$\begin{aligned}
\hat{e}_k^p &= y_d - \hat{y}_k^q \\
&= y_d - \mathcal{M}_k \hat{y}_k^p - \bar{\mathcal{M}}_k \hat{y}_{k-1}^p \\
&= y_d - \mathcal{M}_k (y_k + \eta_k^p) - \bar{\mathcal{M}}_k \hat{y}_{k-1}^p \\
&= y_d - \mathcal{M}_k (H \hat{u}_k + \eta_k^p) - \bar{\mathcal{M}}_k \hat{y}_{k-1}^p \\
&= y_d - \mathcal{M}_k (H u_k + H \eta_k^{pu} + \eta_k^p) - \bar{\mathcal{M}}_k \hat{y}_{k-1}^p
\end{aligned} \tag{39}$$

then (37) is converted to

$$\begin{aligned}
J^p(u_k) &= \frac{1}{4} \|\hat{e}_k^p\|^2 \\
&= \frac{1}{4} \left\| y_d - \mathcal{M}_k (H u_k + H \eta_k^{pu} + \eta_k^p) - \bar{\mathcal{M}}_k \hat{y}_{k-1}^p \right\|^2 \\
&\leq \frac{1}{4} (2 \|y_d - \mathcal{M}_k H u_k - \bar{\mathcal{M}}_k \hat{y}_{k-1}^p\|^2 + 2 \|\mathcal{M}_k H \eta_k^{pu} + \mathcal{M}_k \eta_k^p\|^2) \\
&\leq \frac{1}{2} \|y_d - \mathcal{M}_k H u_k - \bar{\mathcal{M}}_k \hat{y}_{k-1}^p\|^2 + \frac{1}{2} \|\mathcal{M}_k H\|^2 N + \frac{1}{2} \|\mathcal{M}_k\|^2 N
\end{aligned} \tag{40}$$

for (40), the partial derivative of u_k is obtained

$$\begin{aligned}
\frac{\partial J^p(u_k)}{\partial u_k} &= -H^T \mathcal{M}_k (y_d - \mathcal{M}_k H u_k - \bar{\mathcal{M}}_k \hat{y}_{k-1}^p) \\
&= -H^T \mathcal{M}_k (\hat{e}_k^p + \mathcal{M}_k H \eta_k^{pu} + \mathcal{M}_k \eta_k^p)
\end{aligned} \tag{41}$$

then it can be gained

$$u_{k+1} = \hat{u}_k + \beta H^T \mathcal{M}_k (\hat{e}_k^p + H \eta_k^{pu} + \eta_k^p) \tag{42}$$

which completes the proof.

Through (42), it can be seen that the ILC law of the system contains the input and output quantization error terms. Different from the ILC law in Algorithm 1, this control law does not contain the adjustment sequence, which will eventually achieve the bounded convergence of the tracking errors. This will be illustrated by the following Theorem 2.

Theorem 2. *Considering system (15), the ILC law without encoding and decoding mechanism is adopted, if it satisfies*

$$\|I - \beta H H^T P\| \leq \rho_2 < 1 \tag{43}$$

where ρ_2 is a constant, then the expected norm of tracking error achieves bounded convergence

$$\lim_{k \rightarrow \infty} \|E \{e_{k+1}\}\| = \frac{b_1}{1 - \rho_2} \tag{44}$$

where $b_1 = \|H\| \sqrt{N} + \beta \sqrt{N} \|H H^T\| \|H\|$, and the learning gain step β satisfies

$$0 < \beta < \frac{2}{\|H H^T\|} \tag{45}$$

Proof 4. See Appendix.

Different from the ILC law combined with the encoding and decoding mechanism, the ILC law directly quantifying the input and output signals makes the expected norm of the system tracking error converge to a bounded value.

4 Simulation

In this section, the rationality and effectiveness of the proposed algorithm are verified by a joint moving in the horizontal plane of the industrial SCARA robot SEIKOTT3000 in Zhang et al. (2014). Controller-to-actuator and actuator-to-controller data are transmitted over a network with communication bandwidth constraints. Therefore, to minimize the burden of network transmission, the signals are quantified by a uniform quantizer before transmission. The nominal model of the closed-loop joint is

$$G_p(s) = \frac{948}{s^2 + 42s + 948} \quad (46)$$

discretize the above open-loop transfer function, set the sampling time to $T_s = 0.01s$, and the discrete state space model matrices can be obtained as follows

$$A = \begin{bmatrix} 0.6213 & -0.2381 \\ 0.2572 & 0.9589 \end{bmatrix}, B = \begin{bmatrix} 0.0322 \\ 0.0055 \end{bmatrix}, C = [0 \quad 7.4063]$$

The design goal of this paper is to track the desired trajectory with a running time of t , $t \in [0, 2]$ in 30 trials. The desired trajectory adopted is

$$y_d = 5\sin(10\pi t/5) + \sin(10\pi t/10) \quad (47)$$

In the simulation, the “rand” function is used to generate a random sequence in each trial, and the “if” statement is used to make the random variables of the random sequence satisfy the Bernoulli binary distribution at each time point, but they are independent of each other. Without loss of generality, the probability that the Bernoulli binary random variable is 1 at each time point is set to be equal. In order to observe the robustness of the algorithm to continuous data dropouts, we use the ‘for’ statement to limit data loss between trials, mainly from two situations : discontinuous data loss between adjacent trials and continuous data loss of up to three trials.

As assumed in Assumption 2, the initial state of the system is set as $x_k(0) = 0$, and the initial trial input signals of the system are set as $u_0(t) = 0$, $\forall t \in [0, 2]$. Therefore, the performance requirement of the system is to achieve complete tracking of the desired trajectory after finite trials in finite time. The data dropouts rates in this paper are set as 0, 20% and 40%. It can be concluded from Theorem 1 that when the data dropouts rate is 0, it is the upper limit of the selected controller parameter, so the controller parameters is set as $\beta = 0.46$ and $\beta < 2/\|HH^T\| = 1.9926$ is satisfied. The adjustment sequence b_k is selected as $(0.42)^k$, and the controlled system is simulated over 30 trials.

The simulation below has been divided into four parts for the verification. Firstly, we compare the influence of data dropouts rate on tracking performance under different data dropouts rates. Secondly, the two algorithms designed in this paper are compared by simulation to verify the superiority of the proposed design. Then, the simulation is carried out for different data dropouts conditions to illustrate the influence of data dropouts on network communication. Finally, compared with P-type ILC, the effectiveness of the proposed algorithm is verified.

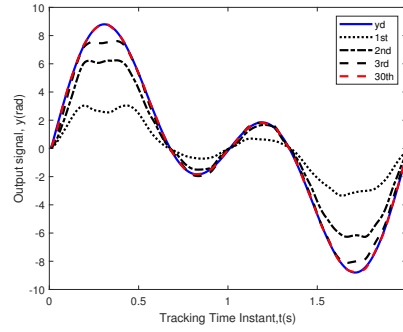


Figure 3: The first few and last trials actual output trajectories of the system with a data dropouts rate of 20%.

In this paper, the output signals y_k , \hat{y}_k of the controller and decoder are called the actual output and the measured output of the system, respectively. Taking the data dropouts rate of 20% as an example to further reflect the effectiveness of the proposed algorithm. Fig. 3 shows the actual output signals' profiles of the designed ILC update law in the first few trials and the 30th trial. The irregular parabola in Fig. 3 is affected by data dropouts and the output gradually tracks the desired trajectory y_d along trials, indicating that in the system with data dropouts, the quantization ILC update law based on the encoding and decoding scheme can achieve completely tracking of y_d .

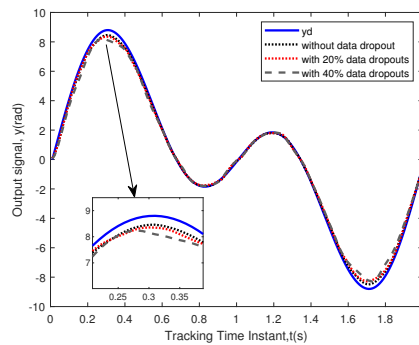


Figure 4: The actual output trajectories of the 5th trial of the system with different data dropouts rates.

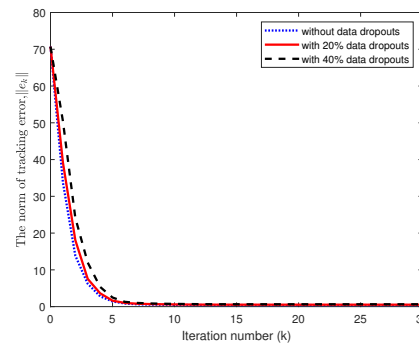


Figure 5: The system tracking error comparison under the data dropouts rate of 0, 20% and 40%.

Theorem 1 only verifies the convergence under different data dropouts rates, but does not verify the convergence speed. Considering the tracking effect of the system output on the desired trajectory under different data dropouts rates, Fig. 4 shows the tracking effect of the 5th trial with data dropouts rates of 0%, 20%, and 40% under the mechanism of discontinuous data dropouts in adjacent trials, and it can be seen that all cases show a high degree of proximity to the desired trajectory. By amplifying the local graph, we can obtain that the proposed algorithm is still effective, but as the data dropouts rate increases, the convergence speed slows down.

Next, in order to consider the impact of different data dropouts rates on the tracking performance of the system, we consider the tracking error simulation under these three data dropouts rates which is shown in Fig. 5. Obviously, the tracking error lines converge to zero and the larger the data dropouts rate, the slower the convergence speed of the algorithm.

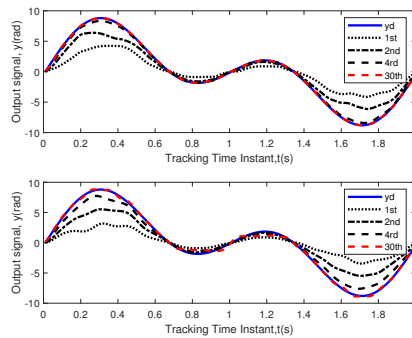


Figure 6: The comparison of the actual output trajectories of the two algorithms under the data dropouts rate of 20%.

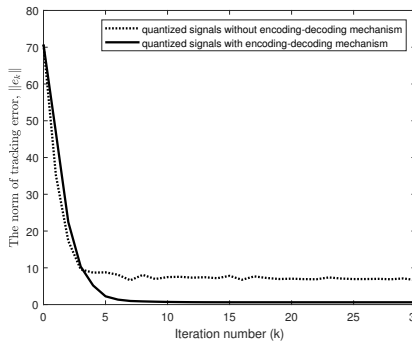


Figure 7: The norm of the expected error of the two algorithms under the data dropouts rate of 20%.

We select the same learning gain β to compare the two quantization strategies, and the simulation effect is shown in Fig. 6 and Fig. 7. Fig. 6 shows the actual output trajectories of the two algorithms under the data dropouts rate of 20%. We can clearly see that the algorithm based on the encoding and decoding mechanism has better convergence effect at the 30th trial. This point can also be obtained in the tracking error lines shown in Fig. 7, indicating that direct quantization of the signal without the encoding and decoding mechanism can only achieve bounded convergence, which verifies our derivation process. Meanwhile, the performance index comparison profiles of the two quantization strategies are drawn in Fig. 8, which are similar to the comparison profile results of the tracking error. The effectiveness of the proposed algorithm is verified.

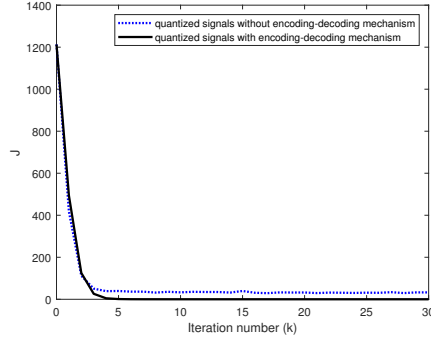


Figure 8: The performance index profiles of two quantization strategies.

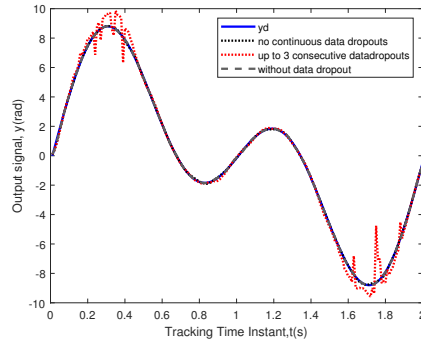


Figure 9: The measured output trajectories of the 10th trial under different data dropouts conditions.

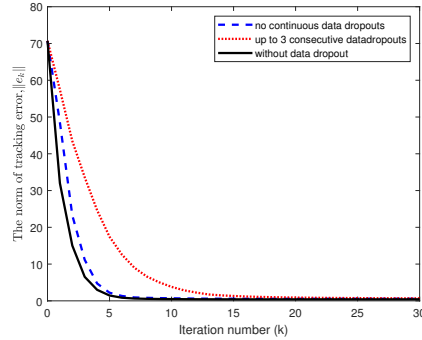


Figure 10: The tracking error lines under different data dropouts conditions.

According to the convergence analysis of Section “ILC Design”, we can get that the number of continuous data dropouts has no effect on the convergence analysis. We will verify the influence of the number of continuous data dropouts on the system through the simulation results. In general, in the case of the same data dropouts rate, the more consecutive data dropouts times, the worse the convergence. We have compared three data dropouts situations: no data dropouts, no data dropouts at different adjacent trials and up to three consecutive data dropouts. When the data dropouts rate is large, the generated random sequence is more likely to be lost multiple times in a row. Fig. 9 and Fig. 10 show the measured output trajectories and tracking error lines of the system under the data dropouts rate of 40%. It can be gotten that the convergence effect of up

to three consecutive data packet dropouts is significantly worse than other cases which verifies our conjecture. Nevertheless, the proposed algorithm can still guarantee the convergence of the system.

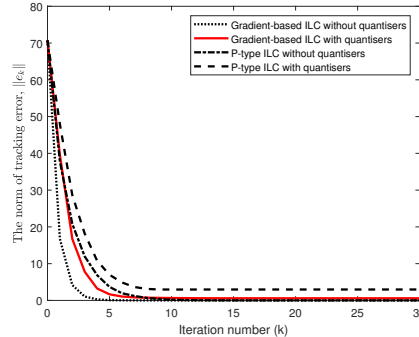


Figure 11: The tracking error of the four schemes under the data dropouts rate of 20%.

Choosing the P-type ILC in [Huang et al. \(2019\)](#) for comparison. The P-type ILC with quantizers and without quantizers is compared with the control law proposed in this paper. These methods are carried out under the same data dropouts rate. Then, the tracking error profiles under the proposed algorithm and the other three methods are shown in Fig. 11. It can be noted in Fig. 11 that the gradient-based ILC has faster convergence speed and better convergence accuracy. Although the quantization has an impact on the tracking performance of the system, the proposed algorithm can obtain an error profile that is approximately coincident with the ILC algorithm without quantizers, indicating the effectiveness of the proposed algorithm.

5 Conclusion

In this paper, the zero-error tracking problem under conditions of data dropouts on the measurement side is studied for networked control systems with limited transmission bandwidth. Under the framework of ILC, two gradient-based ILC laws are designed. When the signals are directly quantized, the tracking error in the sense of mathematical expectation is bounded convergence. The second design is based on the encoding and decoding mechanism to quantify the signals. In this case, the tracking error in the sense of mathematical expectation can be proved to converge to zero, which proves the effectiveness of the algorithm designed in this paper. Simulation results indicate that the proposed scheme can effectively compensate the influence of random data dropouts. Future research will focus on other impacts caused by communication constraints, such as communication delay.

6 Declaration of conflicting interests

The author(s) declared no potential conflicts of interest with respect to the research, authorship, and/or publication of this article.

7 Funding

The author(s) disclosed receipt of the following financial support for the research, authorship, and/or publication of this article: This work was supported by the National Natural Science Foundation of China (Grant Nos. 61773181, 61203092, 62103293); the 111 Project (Grant No. B23008); the Fundamental Research Funds for the Central Universities (Grant No. JUSRP51733B); the Serbian Ministry of Education, Science and Technological Development (Grant No. 451-03-9/2021-14/200108); the National Science Centre in Poland (Grant No. 2020/39/B/ST7/01487); the Natural Science Foundation of Jiangsu Province (Grant No. BK20210709).

References

- Arimoto S, Kawamura S, and Miyazaki F (1984). Bettering operation of robots by learning. *Journal of Robotic Systems* 1(2): 123-140.
- Bahreini M, Zarei J, Razavi-Far R, et al. (2022). Robust and reliable output feedback control for uncertain networked control systems against actuator faults. *IEEE Transactions on Systems, Man, and Cybernetics: Systems*, 52(4), 2555-2564.
- Bu X, Hou Z, Cui L, Yang J. (2017). Stability analysis of quantized iterative learning control systems using lifting representation. *International Journal of Adaptive Control and Signal Processing*, 31(9), 1327-1336.
- Bu X, Wang T, Hou Z, et al. (2015). Iterative learning control for discrete-time systems with quantised measurements. *IET Control Theory & Applications*, 9(9), 1455-1460.
- Chang X, Jin X. (2022). Observer-based fuzzy feedback control for nonlinear systems subject to transmission signal quantization. *Applied Mathematics and Computation*, 414, 126657.
- Choi Y H, Yoo S J. (2020). Quantized feedback adaptive command filtered backstepping control for a class of uncertain nonlinear strict-feedback systems. *Nonlinear Dynamics*, 99(4), 2907-2918.
- Gao L, Liao X, Li H, et al. (2015). Event-triggered control for multi-agent network with limited digital communication. *Nonlinear Dynamics*, 82, 1659-1669.
- Guan S, Zhuang Z, Tao H, et al. (2023). Feedback-aided PD-type iterative learning control for time-varying systems with non-uniform trial lengths. *Transactions of the Institute of Measurement and Control*, 45, 2015-2026.
- Huang L, Ding H, Zhang Z, et al. (2019). A comparison of compensation methods for random input data dropouts in networked iterative learning control system. *Advances in Difference Equations*, 2019(1), 1-16.
- Huang L, Sun L, Wang T, et al. (2022). Optimal input filtering for networked iterative learning control systems with packet dropouts and channel noises in both sides. *International Journal of Robust and Nonlinear Control*, 32(9), 5086-5104.

- Li Z, Chang X, Park J H. (2021). Quantized static output feedback fuzzy tracking control for discrete-time nonlinear networked systems with asynchronous event-triggered constraints. *IEEE Transactions on Systems, Man, and Cybernetics: Systems*, 51(6), 3820-3831.
- Liu W, Chi R. (2021). Iterative learning control for nonlinear nonaffine networked systems with stochastic noise in communication channels. *Transactions of the Institute of Measurement and Control*, 43(14), 3158-3168.
- Patan K, Patan M. (2020). Neural-network-based iterative learning control of nonlinear systems. *ISA transactions*, 98, 445-453.
- Ren Y, Hou Z, Sirmatel I I, et al. (2020). Data driven model free adaptive iterative learning perimeter control for large-scale urban road networks. *Transportation Research Part C: Emerging Technologies*, 115, 102618.
- Shen D, Xu J. (2016). A novel Markov chain based ILC analysis for linear stochastic systems under general data dropouts environments. *IEEE Transactions on Automatic Control*, 62(11), 5850-5857.
- Shen D, Xu J. (2017). A framework of iterative learning control under random data dropouts: Mean square and almost sure convergence. *International Journal of Adaptive Control and Signal Processing*, 31(12), 1825-1852.
- Shen D, Zhang C. (2022). Zero-error tracking control under unified quantized iterative learning framework via encoding–decoding method. *IEEE Transactions on Cybernetics*, 52(4), 1979-1991.
- Shibani, B, Ambure, P, Purohit, A, Suratia, P, et al. (2023). Control of batch pulping process using data-driven constrained iterative learning control. *Computers & Chemical Engineering*, doi: 10.1016/j.compchemeng.2023.108138.
- Tang J, Sheng L. (2018). Iterative learning fault-tolerant control for networked batch processes with event-triggered transmission strategy and data dropouts. *Systems Science & Control Engineering*, 6(3), 44-53.
- Wang W, Ma J, Li X, Cheng Z, et al. (2020). Iterative super-twisting sliding mode control for tray indexing system with unknown dynamics. *IEEE Transactions on Industrial Electronics*, 68(10), 9855-9865.
- Xu Y, Shen D, Bu X. (2017). Zero-error convergence of iterative learning control using quantized error information. *IMA Journal of Mathematical Control and Information*, 34(3), 1061-1077.
- Yang H, Xu H, Xia Y, et al. (2020). Stability analysis on networked control systems under double attacks with predictive control. *International Journal of Robust and Nonlinear Control*, 30(4), 1549-1563.
- Yu H, Chen T. (2023). Periodic event-triggered networked control systems subject to large transmission delays. *IEEE Transactions on Automatic Control*, 68(1), 63-79.
- Zhang B, Ye Y, Zhou K, and Wang D. (2014). Case studies of filtering techniques in multirate iterative learning control. *Control Engineering Practice*, 26, 116-124.

Zhang C, Shen D. (2018). Zero-error convergence of iterative learning control based on uniform quantisation with encoding and decoding mechanism. *IET Control Theory & Applications*, 12(14), 1907-1915.

Zhang H, Chi R, Hou Z, Huang B. (2022). Data-driven iterative learning control using a uniform quantizer with an encoding–decoding mechanism. *International Journal of Robust and Nonlinear Control*, 32(7), 4336-4354.

Zhang Z, Liang H, Wu C, et al. (2019). Adaptive event-triggered output feedback fuzzy control for nonlinear networked systems with packet dropouts and actuator failure. *IEEE Transactions on fuzzy Systems*, 27(9), 1793-1806.

8 Appendix

8.1 Proof of Theorem 1

Denote $e_{k+1} = y_d - y_{k+1} = y_d - H\hat{u}_{k+1}$, From (22), it can be gained

$$\hat{e}_{k+1} = \mathcal{M}_{k+1}e_{k+1} - \mathcal{M}_{k+1}b_{k+1}\eta_{k+1}^y + \bar{\mathcal{M}}_{k+1}\hat{e}_k \quad (48)$$

then, it can be concluded that

$$\mathcal{M}_{k+1}e_{k+1} = \hat{e}_{k+1} + \mathcal{M}_{k+1}b_{k+1}\eta_{k+1}^y - \bar{\mathcal{M}}_{k+1}\hat{e}_k \quad (49)$$

from the control law (31) and (17), it can be obtained

$$\begin{aligned} e_{k+1} &= e_k + H\hat{u}_k - H\hat{u}_{k+1} \\ &= e_k + H\hat{u}_k - H(u_{k+1} + b_k\eta_{k+1}^u) \\ &= e_k + H\hat{u}_k - Hb_k\eta_{k+1}^u - H(\hat{u}_k + \beta H^T \mathcal{M}_k(\hat{e}_k + Hb_{k-1}\eta_k^u + b_k\eta_k^y)) \\ &= (I - \beta H H^T \mathcal{M}_k) e_k - \beta H H^T \mathcal{M}_k H b_{k-1} \eta_k^u - H b_k \eta_{k+1}^u \end{aligned} \quad (50)$$

due to \mathcal{M}_k is a diagonal matrix composed of N random factors $w_k(t)$ independent of e_k and u_k . then taking expectations on both sides of (50)

$$E\{e_{k+1}\} = (I - \beta H H^T P) E\{e_k\} - \beta H H^T P H b_{k-1} \eta_k^u - H b_k \eta_{k+1}^u \quad (51)$$

since P is composed of ω_t satisfying $0 < \omega_t < 1$, we can obtain $\|P\| < 1$. By taking norms on both sides of the last equation gives

$$\begin{aligned} \|E\{e_{k+1}\}\| &\leq \|I - \beta H H^T P\| \|E\{e_k\}\| + \|\beta H H^T P H b_{k-1} \eta_k^u\| + \|H b_k \eta_{k+1}^u\| \\ &\leq \|I - \beta H H^T P\| \|E\{e_k\}\| + \|\beta H H^T\| \|H\| \sqrt{N} b_{k-1} + \|H\| \sqrt{N} b_k \end{aligned} \quad (52)$$

When the appropriate learning gain β is chosen such that $\|I - \beta H H^T P\| \leq \rho_1 < 1$ holds, and the adjustment sequence $b_k = \tau^k$, $0 < \tau < 1$ holds, then

$$\|E\{e_{k+1}\}\| \leq \rho_1 \|E\{e_k\}\| + c b_k \quad (53)$$

where $c = \sqrt{N} \left(\frac{\|\beta HH^T\| \|H\|}{\tau} + \|H\| \right)$. The recursive formula of the actual tracking error obtained by the system after k trials is

$$\begin{aligned} \|E\{e_{k+1}\}\| &\leq \rho_1^{k+1} \|E\{e_0\}\| + c \sum_{i=0}^k \rho_1^i b_{k-i} \\ &= \rho_1^{k+1} \|E\{e_0\}\| + c \sum_{i=0}^k \rho_1^i \tau^{k-i} \end{aligned} \quad (54)$$

since $\lim_{k \rightarrow \infty} \rho_1^{k+1} = 0$, $\lim_{k \rightarrow \infty} \sum_{i=0}^k \rho_1^i \tau^{k-i} = 0$, and $c = \sqrt{N} \left(\frac{\|\beta HH^T\| \|H\|}{\tau} + \|H\| \right)$, it can be further obtained

$$\lim_{k \rightarrow \infty} \|E\{e_{k+1}\}\| = 0 \quad (55)$$

On the basis of $\|I - \beta HH^T P\| \leq \rho_1 < 1$, it can be gained

$$0 < \|\beta HH^T P\| < 2 \quad (56)$$

since $CB \neq 0$, it can be gotten that H is a positive definite matrix, and P is a bounded diagonal matrix composed of ω_t satisfying $0 < \omega_t < 1$, then we can see that $HH^T P$ is also a positive definite matrix. The final formula (56) can be converted to

$$0 < \beta < \frac{2}{\|HH^T P\|} \quad (57)$$

and $\|HH^T P\| \leq \|HH^T\| \|P\| < \|HH^T\|$, we can further get

$$0 < \beta < \frac{2}{\|HH^T\|} \quad (58)$$

which completes the proof.

8.2 Proof of Theorem 2

By $\hat{e}_{k+1}^p = y_d - \hat{y}_{k+1}^q$, combining (34) and (36), it can be obtained

$$\begin{aligned} \hat{e}_{k+1}^p &= y_d - \hat{y}_{k+1}^q \\ &= y_d - \mathcal{M}_{k+1} \hat{y}_{k+1}^p - \bar{\mathcal{M}}_{k+1} \hat{y}_k^p \\ &= y_d - \mathcal{M}_{k+1} (y_{k+1} + \eta_{k+1}^p) - \bar{\mathcal{M}}_{k+1} (y_k^p + \eta_k^p) \\ &= \mathcal{M}_{k+1} e_{k+1} + \bar{\mathcal{M}}_{k+1} e_k - \mathcal{M}_{k+1} \eta_{k+1}^p - \bar{\mathcal{M}}_{k+1} \eta_k^p \end{aligned} \quad (59)$$

It can be derived from the control laws (38) and (17) that

$$\begin{aligned} e_{k+1} &= e_k + H \hat{u}_k - H \hat{u}_{k+1} \\ &= e_k + H \hat{u}_k - H (u_{k+1} + \eta_{k+1}^{pu}) \\ &= e_k + H \hat{u}_k - H (\hat{u}_k + \beta H^T \mathcal{M}_k (\hat{e}_k^p + H \eta_k^{pu} + \eta_k^p) + \eta_{k+1}^{pu}) \\ &= e_k - H \eta_{k+1}^{pu} - \beta H H^T \mathcal{M}_k (H \eta_k^{pu} + \eta_k^p) \\ &\quad - \beta H H^T \mathcal{M}_k (e_k + \bar{\mathcal{M}}_k e_{k-1} - \eta_k^p - \bar{\mathcal{M}}_k \eta_{k-1}^p) \\ &= (I - \beta H H^T \mathcal{M}_k) e_k - H \eta_{k+1}^{pu} - \beta H H^T \mathcal{M}_k H \eta_k^{pu} \end{aligned} \quad (60)$$

taking expectation on both sides of (60), it can be obtained

$$E \{e_{k+1}\} = (I - \beta H H^T P) E \{e_k\} - H E \{\eta_{k+1}^{pu}\} - \beta H H^T P H E \{\eta_k^{pu}\} \quad (61)$$

and taking the norm on both sides of (61) gives

$$\|E \{e_{k+1}\}\| \leq \|I - \beta H H^T P\| \|E \{e_k\}\| + \|H\| \sqrt{N} + \beta \|H H^T\| \|H\| \sqrt{N} \quad (62)$$

next define

$$b_1 = \|H\| \sqrt{N} + \beta \|H H^T\| \|H\| \sqrt{N} \quad (63)$$

and then

$$\|E \{e_{k+1}\}\| \leq \rho_2 \|E \{e_k\}\| + b_1 \quad (64)$$

The following inequality can be gotten after k trials of the last formula

$$\|E \{e_{k+1}\}\| \leq \rho_2^k \|E \{e_0\}\| + \frac{1 - \rho_2^{k+1}}{1 - \rho_2} b_1 \quad (65)$$

applying $\lim_{k \rightarrow \infty} \rho_2^k = 0$ to (62), we obtain

$$\lim_{k \rightarrow \infty} \|E \{e_{k+1}\}\| = \frac{b_1}{1 - \rho_2} \quad (66)$$

and the proof is completed.